A storyline of ozone pollution extremes in warmer climates

Tamara Emmerichs

tamara.emmerichs@gmx.de

Forschungszentrum Jülich GmbH https://orcid.org/0000-0002-0165-9574

Fuzhen Shen

Forschungszentrum Jülich GmbH

Sergey Gromov

Max-Planck Institute for Chemistry

Michaela Hegglin

Juelich https://orcid.org/0000-0003-2820-9044

Andreas Wahner

Forschungszentrum Juelich GmbH https://orcid.org/0000-0001-8948-1928

Domenico Taraborrelli

Forschungszentrum Jülich GmbH

Article

Keywords: Tropospheric ozone, air pollution, premature mortality, storyline scenarios, climate change

Posted Date: April 22nd, 2024

DOI: https://doi.org/10.21203/rs.3.rs-4208627/v1

Additional Declarations: (Not answered)

A storyline of ozone pollution extremes and their impacts in warmer climates

Tamara Emmerichs[1*], Fuzhen Shen[2], Sergey Gromov[3], Michaela I. Hegglin[2,4], Andreas Wahner[1] and Domenico Taraborrelli[1,5]

[1*]Institute of Energy and Climate Research: Troposphere (IEK-8), Forschungszentrum Jülich GmbH, Jülich, Germany.
[2]Institute of Energy and Climate Research: Stratosphere (IEK-7), Forschungszentrum Jülich GmbH, Jülich, Germany.
[3]Max-Planck Institute for Chemistry, Mainz, Germany.
[4]Department of Meteorology, University of Reading, Reading, United Kingdom.
[5]Center for Advanced Simulation and Analytics (CASA), Forschungszentrum Jülich GmbH, Jülich, Germany.

*Corresponding author(s). E-mail(s): t.emmerichs@fz-juelich.de;
Contributing authors: f.shen@fz-juelich.de;
sergey.gromov@mpic.de; m.i.hegglin@fz-juelich.de;
a.wahner@fz-juelich.de; d.taraborrelli@fz-juelich.de;

Abstract

High ozone levels pose a significant threat to human health and ecosystems, especially during extreme weather events. These are expected to become more frequent and intense with climate change, exacerbating the interactions between weather, vegetation, and air pollution. Traditionally a climate change penalty is expected for ground-level ozone is expected. However, models do not even agree on the sign of the change over most of the continents suggesting an important role for vegetation. We address this uncertainty by incorporating realistic vegetation responses to abiotic stress into a global atmospheric chemistry model. We develop novel storyline scenarios of air pollution, contrasting the actual climate of 2018-2020 with two different levels of warming. Our results show that under warming, vegetation and local photochemistry generally conspire to exacerbate ozone pollution extremes, while

a concurrent moistening of the free troposphere leads to a lower ozone background. The competition between these two effects depends on the degree of warming and will determine whether climate change results in a penalty or a benefit. However, the role of changing pollutant emissions remains uncertain and should be addressed in future studies.

Keywords: Tropospheric ozone, air pollution, premature mortality, storyline scenarios, climate change

1 Introduction

Ozone (O_3) has adverse effects on human health [1] and damages vegetation reducing ecosystem productivity and crop yields [2]. In the troposphere, it is produced photochemically and is a key driver of the atmospheric oxidation capacity [3]. The regional distribution of ground-level O_3 is influenced by precursor emissions, vegetation uptake, and photochemistry, all of which dependent on meteorological conditions [4].

Over the continents, positive correlations of O_3 with temperature are usually found [5, 6]. However, correlations with humidity may have different signs depending on the local chemical and land-atmosphere coupling regimes [7]. Dry deposition to vegetation, a major sink of O_3, as well as biogenic emissions of its precursors are strongly modulated by meteorology as plants respond to drought and heat stress [8, 9]. Despite this knowledge, Earth system models are still largely inconsistent about the land-atmosphere-chemistry coupling on continental ground-level O_3 under climate change [10].

The assessment of future O_3 pollution changes due to climate change has so far relied on the classical probabilistic (risk-based) approach using ensembles of model simulations [10, 11]. However, this method is limited by the uncertainty associated with the atmospheric circulation aspects of climate change such as shifts in the polar jet stream [12]. In contrast, storyline scenarios primarily address the thermodynamic aspects of climate change [13]. In storyline simulations, the dynamics of the model (including large-scale winds and vorticity) are prescribed with reanalysis data, allowing the reproduction of recent extreme events and the quantification of the response of Earth system processes under changed thermodynamic conditions. Anthropogenic emissions are fixed to keep the focus of the study on thermodynamic aspects.

During the summers of 2018, 2019, and 2020, large parts of Europe experienced exceptional heat waves, breaking several records. The intensity, persistence and spatial extent of the 2018 summer heatwave was comparable to the 2003 'mega-heatwave' [14]. The year 2019 saw the highest ever recorded temperatures across Europe, while 2020 was one of the three warmest years on record [15, 16]. In addition, the occurrence of severe droughts in 2018 was not limited to central Europe, but extended to large parts of the Northern Hemisphere (NH) [14]. The soil moisture-temperature feedback is known to amplify

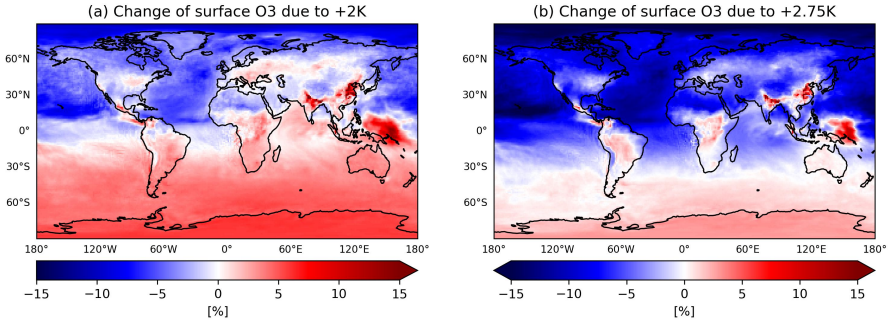

Fig. 1 Multi-year (2018-2020) relative change of daily average ground-level ozone (a) due to the +2K (b) and the +2.75K scenario during the warm spell (June to August).

heatwaves [17] and has been shown to intensify the one during summer 2018 in Europe [18]. In addition, vegetation feedbacks in this region are known to exacerbate extreme ozone pollution [19].

This study provides, for the first time, global storylines of air pollution. Using the global atmospheric chemistry model ECHAM/MESSy Atmospheric Chemistry (EMAC) [20], one factual (+1.1K relative to preindustrial) and two sensitivity (+2K, +2.75K relative to preindustrial) simulations are performed for the years 2018-2020. The novel storyline approach allows us to study how O_3 extremes are affected by climate change, in particular considering thermodynamic changes (warming and moistening) and the role of vegetation-atmosphere interactions.

The results of how the different sensitivity simulations affect ground-level ozone levels are presented in section 2.1. The drivers of future O_3 extremes are discussed in Sec. 2.2. Sec. 2.3 re-evaluates the O_3-climate penalty and contrasts our results with the body of recent literature. We also consider the change in various O_3 pollution metrics in the storylines (Sec. 2.4) and the detrimental effects on humans and terrestrial vegetation (Sec. 2.5). The paper concludes with summarising the main results and discussing the storyline approach, the remaining O_3 bias, and the role of vegetation.

2 Results

2.1 Ozone in warmer climates

Figure 1 shows the predicted change in ground-level O_3 for two warming scenarios relative to the period 2018-2020. A higher global mean temperature of 2K (Fig. 1a) leads to an increase of up to 10 % in mean ground-level ozone during the boreal summer (June to August, daily averages) in the most populated regions of the NH, with the largest positive changes occurring in East Asia. Note that the high relative increase in the equatorial Pacific Ocean only

reflects a minimum in absolute values of O_3 in this area (Fig. S4) [21]. Background levels of O_3 in the northernmost regions, especially over the oceans, decrease by 5-10 %.

In the +2.75K world, these ozone reductions become more pronounced, with decreases of up to 15 % over the oceans and extending to larger regions, including the equatorial region of the Southern hemisphere (SH). On average, this change exceeds the internal model variability of daily O_3 which is higher in 30°S-30°N than in the high NH latitudes (standardised mean difference: Fig. S1-S3). While at +2K large ozone increases >10 % are found on the SH, at +2.75K the changes are much smaller <5 % with positive values occurring uniformly over the extra tropics and only over the land in the equatorial region.

Globally, the 2.75K warming results in a reduction of the tropospheric ozone burden by about 20 Tg relative to the factual climate (371 Tg, in 2018 Tab. A.1). These results are in contrast to the recent findings by [22], who found an increase in the future ozone burden from the CMIP6 simulations (classical probabilistic approach, ssp370 pathway), mainly due to changes in pollutant emissions and inflow from the stratosphere.

2.2 Drivers of ground-level ozone

The changes in ground-level O_3 in the two warming scenarios are here explained by the evolution of the two main drivers: dry deposition and net chemical effect. We target the relevant timescales for local ozone by analysing the daily accumulated values of dry deposition fluxes and chemical tendency diagnosed with passive tracers (Sec. A.1). The general change patterns are similar for all three years.

In general, ground-level O_3 production exceeds the chemical loss in most regions, except in northeastern China and India, where the loss term dominates. In warmer climates, local drivers over the continents push towards higher levels of ground-level ozone. For example, in the eastern USA and East Asia, the net O_3 chemistry at ground level is by up to 10 ppb/d higher in the +2.75K scenario during the boreal summer (see Fig. 2a). Higher temperatures favour the radical chemistry that drives the O_3 production and is also reflected by the dO_3/dT slope (Fig. 3a). This dominates the increase in chemical loss.

Rising O_3 levels in Europe can be linked to an increase in isoprene emissions from plants (Fig. S5), similar to [5]. This leads to increased RO_2 formation that drives the O_3 production. The inhibition of isoprene emissions by elevated CO_2 concentrations [23] counterbalances this effect in the inner tropics, which is enhanced by the warmer scenario. In other regions, it plays a minor role [24].

During the night, nitrogen oxides emitted from the soil are converted to NO_2 upon reaction with O_3. In warmer climates, emissions increase, leading to a stronger nighttime O_3 consumption, which reduces the chemical O_3 effect in the +2.75K scenario relative to the factual world. This effect is small in the NH, while it compensates for up to 20 % of the diurnal change in the SH (Fig. S7).

Future increases in CO_2 (CO_2-inhibition) reduce the plant activity in the Amazon, Central Africa, and Southeast Asia. In regions of increased humidity, the O_3 uptake at leaf surfaces increases [25].

In a warmer climate (+2.75K), we see a reduction of O_3 deposition in (NH) boreal forests, which is explained by higher O_3-induced stress (20-30 % more damage, see Sec. 2.5.1). Drought stress (+5-10 %) resulting from the temperature increase in the warmer climate [26] further increases the plant sensitivity in the NH and leads to greater vulnerability to O_3 damage. The effect on soil moisture is only very local, so no specific feedback mechanism (e.g. partitioning between soil moisture and energy-limited regime) is seen. Overall, the change in the actual dry deposition flux (Fig. 2b) is dominated by the changes in the O_3 concentrations (Fig. 1b).

In addition to local drivers, background ozone is also an important determinant of ground-level ozone. Background ozone is largely reduced in the +2.75K scenario (Fig. 1b). The changes are most pronounced over the oceans and affect the continents via long-range transport, e.g. from the North Atlantic to Northern Europe [27]. Much of the decrease is due to the enhanced O_3 destruction in the free troposphere (Fig. S6) where, in contrast to the (continental) boundary layer, water vapour is the limiting factor for the $O(^1D)$ loss [28]. This loss term increases by 11.7 % (150 Tg/yr) in the NH and by 6.1 % (154 Tg/yr) globally. This is consistent with findings of widespread decreases in O_3 in warmer and moister climates [10].

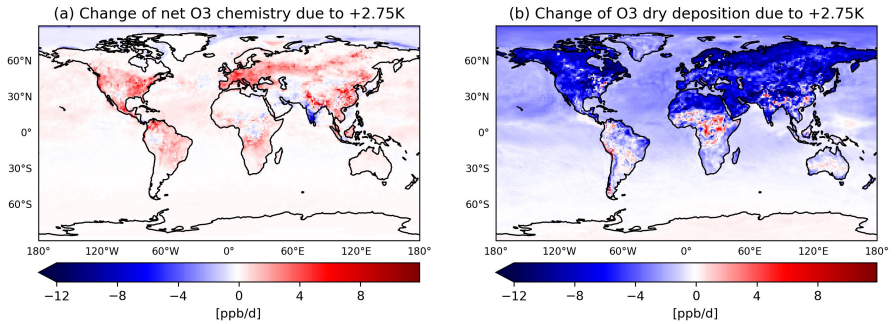

Fig. 2 Absolute change of the daily accumulated (a) net O_3 chemistry at ground level and (b) the O_3 dry deposition due to the +2.75K climate during summer (JJA) 2018.

Thus, the competition between changes in background ozone and changes in local chemical drivers results in the overall change in ground-level ozone.

2.3 Ozone-climate penalty or benefit?

The 'O_3-climate penalty' describes the amplification of O_3 air pollution due to climate warming, defined as the slope of the O_3 change with temperature change. Several estimation methods exist in the literature (e.g. correlation of observed long-term O_3 with temperature, perturbation of temperature) ([29]

and references therein). Here, we use the factual EMAC simulation and the storyline scenario (+2.75K) to reproduce such a measure (Fig. 3). 2m temperature increases in a warmer climate almost over the whole globe (Sec. S1), except in India where a stronger aerosol cooling occurs, especially in the south. The sensitivity of O_3 to temperature changes increases significantly with a maximum of 5 ppb/1K in East and South Asia (Fig. 3a) as it also has been found by [10]. In contrast to their study (ssp370 modified anthropogenic emissions), we explain the increase in dO_3/dT by the sensitivity of the local O_3 to enhanced isoprene emissions which agrees with findings for e.g. China [30]. The positive slope in the USA (Fig. 3a) is consistent with the findings from observations in this region [31]. Over the oceans, we find a negative slope only in the tropical Pacific, in agreement with the CMIP6 model ensemble (ssp370 scenario) [10].

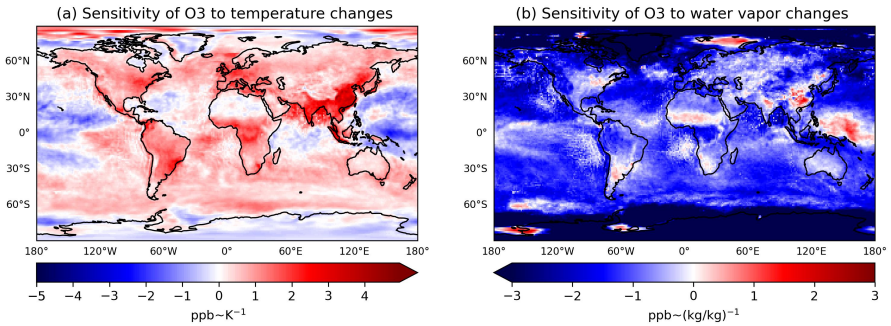

Fig. 3 Multi-year (2018-2020) sensitivity of O_3 changes to (a) temperature changes (regression coefficient dO_3/dT in [ppb/K]) (b) and dO_3/dH_2O [ppb/kg kg^{-1}] at ground level.

The increases of future atmospheric water vapour particularly affects the chemistry in the free troposphere [28]. The dO_3/dH_2O slope over North America shows a N-S gradient consistent with observations by [31] and can be explained by a shift in the land-atmosphere coupling regime (from soil water-limited to energy-limited regime) [7]. The same reason may also apply to East Asia: The positive slope there reflects the shift to a NO_x-limited regime [32]. The equatorial Pacific Ocean is probably related to the moist convection that transports O_3 downwards [33].

Although the assessment of the future O_3 sensitivities reveals a significant increase in O_3 production with rising temperature (commonly known as 'climate penalty') we show here the additional importance of the O_3 sensitivity to water vapour. This effect tends to result in a regional 'climate benefit'. However, we note that additional meteorological covariances with other biosphere-related phenomena (e.g. soil NO_x emissions) may contribute significantly to the O_3-temperature correlation. For example, [34] attribute as much as 60 % of the O_3-temperature relationship to these factors.

2.4 Ozone pollution extremes

There are several metrics that define O_3 extremes, two of which are shown here. While the daily maximum 1-hour daily O_3 (MHM1O_3) captures the short-term variability due to chemical ozone production and loss, governments often refer to the 8-hour daily maximum running mean of O_3 (MDA8O_3, e.g. the World Health Organisation guidelines [35] threshold: 50 ppb) as a guideline. MDA8O_3 takes into account the relevant human exposure time to O_3 and varies with factors such as dry deposition [1].

Under present-day conditions (*factual*, equivalent to a +1.1K vs. pre-industrial), the highest number of MHM1O_3 (exceeding 90 ppb) occurs between 90 and 100 ppb in the four regions (first four histograms in Fig. 4) with a maximum of 1750 events in East Asia. The number of extremes decreases exponentially with increasing level down to values of 125 ppb (log-normal distribution). A significantly higher number of MDA8O_3 events than MHM1O_3 events occur in Europe, indicating the important role of long-range transport, especially in summer when Asian and North American emissions contribute more to European O_3 than regional emissions [27].

In the +2K scenario, the number of MHM1O_3 events increases in all four regions (shown here in the histograms). By far the largest increase in number of extreme events (about 800) is seen in Europe, which can be explained by the strong correlation between O_3 levels and air temperature (see Sec. 2.3). MDA8O_3 extremes increase in Europe and Asia, occurring only at high in Europe and at medium O_3 levels in South Asia due to the different background pollution and chemistry regimes. As the world continues to warm, the O_3 extremes decrease in the NH due to the reduced background ozone transported from distant regions. In areas with sufficiently high temperatures (up to 50° N), this effect is counterbalanced by the increase of net O_3 chemistry (see Sec. 2.2), as seen in Figure 4b . China is an exception, as high O_3 levels in summer mainly occur due to biogenic emissions [36] which increase significantly in the future (see Sec. 2.2, Fig. S5).

2.5 Detrimental effects on humans and plants

Finally, we estimate how structural changes in O_3 pollution would affect plants and human health in a +2K and +2.75K scenario, given the 2018-2020 atmospheric dynamics. It should be noted that the impacts presented below do not take into account the effects of changes in pollutant emissions which remain rather uncertain.

2.5.1 Ozone and terrestrial vegetation

We assess the cumulative O_3 uptake through the stomata, against a dynamic threshold (see section A.1), i.e., the phytotoxic ozone damage (POD). The estimated global distribution with local values reaching 100 mmol$(O_3)/m^2$ is generally in agreement with the estimates by [38–40]. The maxima consistently occur over the tropical forests, however overestimated due to the mismatch

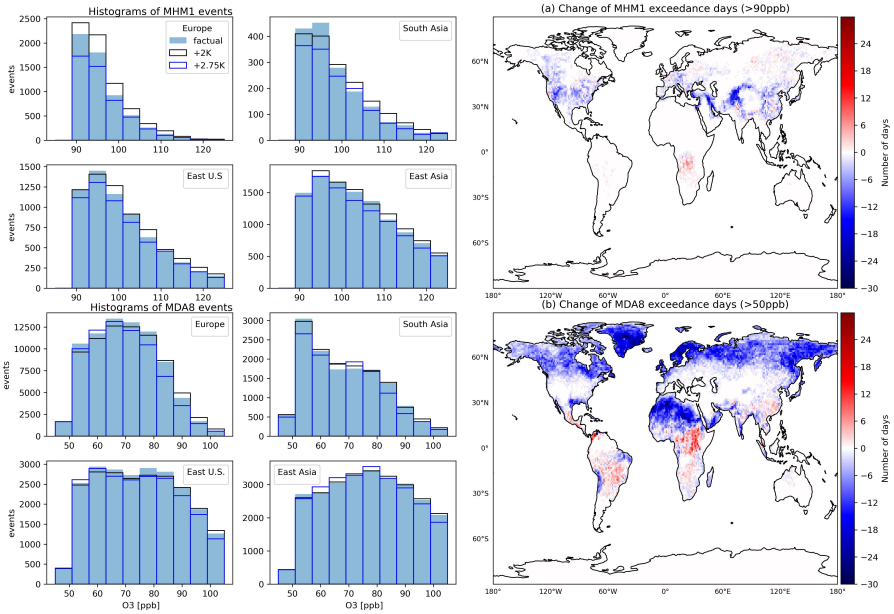

Fig. 4 (top) Number of maximum daily 1-h average ground-level O_3 exceeding 90 ppb (MHM1) in different regions and (a) the global distribution of the absolute change in summer 2018 due to the +2.75K scenario, (bottom) number of daily maximum 8-hourly running mean exceeding 50 ppb in different regions and (b) the global distribution of the absolute change in summer 2018 due to the +2.75K scenario. The regions are defined according to the sixth IPCC assessment report [37]: Europe (16,17,18, only land), S.E. U.S: 5, East Asia: 35, South Asia (SAS): 37.

of the plant types used in the model (see Sec. A.1). In the +2.75K scenario, POD increases significantly in NH forests (Fig. 5b), counteracting the average decrease in summer O_3. The changes in stomatal fluxes are primarily driven by the decrease in atmospheric stability [41] (i.e. increased aerodynamic transport).

2.5.2 Ozone pollution and human health

We also assess human health impacts by estimating premature mortality due to long-term exposure to enhanced O_3 levels. Shown in Figure 6a, the calculated annual total is at 0.14 million O_3 mortality cases, mainly concentrated in China and India, which are the most polluted and densely populated regions of the world. Estimates from alternative studies yield higher global values in 2019 (0.42 million for ozone-attributable chronic respiratory disease, 0.37 million for chronic obstructive pulmonary disease) [42, 43]. This discrepancy may be attributed to the use of a lower relative risk for all-cause mortality [44] than in this study (1.01 vs. 1.06 relative risk) and the use of different ozone thresholds [45]. Furthermore, lower estimates result from the different climate pathway used here (see Sec. A.1) (ssp2.45 vs. ssp3.70: 3.12 million; RCP8.5: 0.32 million) [46, 47]. Compared with the factual world, ground-level ozone in the +2K

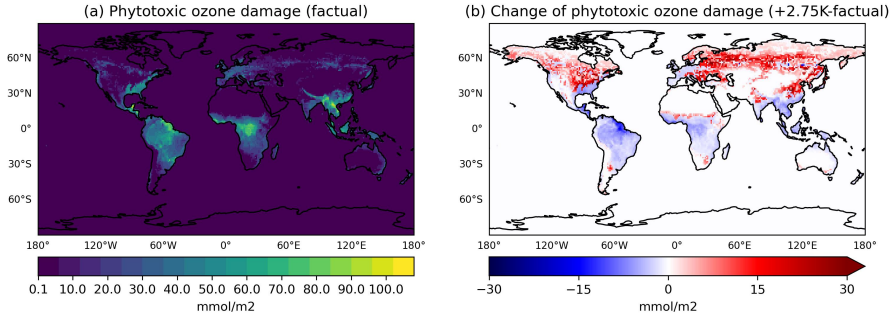

Fig. 5 Multi-year (2018-2020) mean (a) relative crop yield in the +2.75K scenario and (b) the ratio versus factual climate (+1.1K vs. pre-industrial).

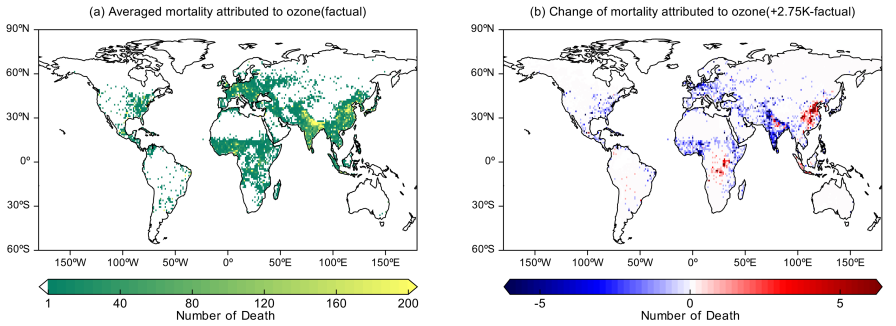

Fig. 6 Multi-year (2018-2020) mean (a) premature mortality in factual (+1.1K vs. pre-industrial) climate and (b) the difference to the +2.75K scenario. (Note: white color in color bar (a) means zero)

scenario (Fig. S8) is estimated to cause more (all-causes) mortality deaths worldwide (2018-2020 average). On the contrary, in the +2.75K scenario, the corresponding number of deaths decreases in most countries, except for China and several African countries (Fig. 6b) due to a widespread decrease in ground-level O_3 (Fig. 1b). In China, the number of excess deaths increases by 375, followed by 83 in the Democratic Republic of the Congo and 19 in Angola. The differences between the two storylines and the factual estimates show that the shift to the warmer scenario significantly reduces the global health burden (Fig. S8 for +2K, and Fig. 6b for +2.75K). In India (the most heavily populated country), the 2018-2020 average total number of avoided premature deaths due to the shift to the +2.75K scenario is 2298, contrasting the figure of 450 in the USA. Although the number of deaths in China increases under the +2.75K scenario compared to the factual climate, this increase is smaller than in the +2K scenario. Globally, the +2.75K scenario allows avoiding 78.2 % of O_3-related deaths.

3 Discussion and Conclusion

This study assesses the evolution of ozone pollution extremes in a warmer world, examining two different storyline scenarios. Our results show that ozone extremes will increase in many parts of the "2K warmer world" due to the amplification of O_3 production by temperature and higher biogenic emissions. In contrast, a warming of 2.75K leads to a dominant increase of the major O_3 loss terms in the NH, resulting in a reduction of O_3 extremes in line with some previous studies (e.g. [10]). Thus, the thermodynamic aspects of extreme global warming above 2K indicate (somewhat unexpected) potential beneficial effects on air quality, reduction of the frequency and intensity of pollution extremes that are harmful to human and vegetation health.

Conducting the first storylines-based air pollution study shows its suitability for extending the knowledge gained from classical predictions. The uncertainties about atmospheric dynamics, a significant source for uncertainty in model-aided climate change studies, are largely avoided in the storyline projections, while the computational effort for the simulations is significantly reduced compared to conventional probabilistic approaches.

The present-day representation of ground-level ozone in our model compares well against a chemical reanalysis product, while models typically show an overestimation of 10 % in the NH [22].

These storylines can be widely used in the community to understand future changes. The plant sensitivities to drought and ozone considered in this study improve the realism of vegetation-atmosphere interactions, which is key to reducing the uncertainty in future air quality and climate studies over the continents. However, to assess the overall change in air pollution in the future, the role of land cover changes (including those driven by expected increases in the frequency and intensity of wildfires) in exacerbating weather and pollution extremes, and the effect of changing anthropogenic emissions, must be included in this framework.

4 Author contribution

DT and TE created the concept of the study. DT and SG developed the approaches for chemical budgeting of ozone. TE implemented several model developments, prepared and conducted the global simulations, analysed the model output and wrote most of the paper. FS estimated the premature mortality related to ozone and the changes in a warmer climate and wrote the respective part of the manuscript with guidance from MIH. AW, MIH, DT, SG and TE reviewed and edited the manuscript.

5 Acknowledgements

The authors gratefully acknowledge the help of Linda van Garderen and Frauke Feser when preparing the synthetic SST data for the storyline simulations.

Simon Rosanka provided the implementation and namelist files for the inclusion of Secondary Organic Aerosols in the model setup. The authors gratefully acknowledge the Gauss Centre for Supercomputing e.V. (www.gauss-centre.eu) for funding this project by providing computing time on the GCS Supercomputer JUWELS [48] and by the John von Neumann Institute for Computing (NIC) and provided on the supercomputer JURECA [49] at Jülich Supercomputing Centre (JSC). The authors gratefully acknowledge the Earth System Modelling Project (ESM) for funding this work by providing computing time on the ESM partition of the supercomputer JUWELS at the Jülich Supercomputing Centre (JSC).

6 Competing interests

All authors declare no financial or non-financial competing interests.

7 Code availability

The Modular Earth Submodel System (MESSy) is continuously further developed and applied by a consortium of institutions. The usage of MESSy and access to the source code is licenced to all affiliates of institutions which are members of the MESSy Consortium. Institutions can become a member of the MESSy Consortium by signing the MESSy Memorandum of Understanding. More information can be found on the MESSy Consortium Website http://www.messy-interface.org. The code used in this study will be included in the devel branch of the MESSy repository.

Appendix A Methods

A.1 Global atmospheric chemistry model

General description

For this study, the global atmospheric chemistry model ECHAM/MESSy is used which consist of the fifth-generation European Centre Hamburg general circulation model [ECHAM5,version 5.3.02; 50] as the atmospheric general circulation model. MESSy provides a flexible infrastructure with more than 30 different submodels representing chemical, physical and biogeochemical processes for coupling processes to build comprehensive Earth system models (ESMs). The gas-phase chemistry is based on a comprehensive mechanism (200 reactions) as used in the EMAC simulations for the Chemistry-Climate Model Intercomparison Project (CCMI2) [51, 52]. Passive tracers are created with a tagging tool and are used for budgeting the chemical production and loss of ozone [53]. A set of two passive tracers tracking the total production and loss of O_3 is used to diagnosed the exact net chemical tendency (see Sec. 2.2). The global annual budget of odd oxygen is calculated from a different set of

passive tracers (see Tab. S1). The aerosol scheme simulates black carbon, particulate organic matter, dust, sea spray, sulfate and ammonium aerosol among others [GMXE; 54]. A simplified scheme for secondary organic aerosols from major precursors is included [55].

Emissions

The anthropogenic emissions are branched off from the EMAC CCMI2 simulation output for the respective periods. (greenhouse gases: CO_2, CH_4, N_2O etc.) The simulated mixing ratios of long-lived species (greenhouse gases: CO_2, CH_4, N_2O etc.) at the lowest model layer are assimilated via Newtonian relaxation (every 3 hours) to projected mixing ratios branched off from the EMAC CCMI2 simulation output. The lightning emissions of nitrogen oxides (NO) are based on the correlation between the convective cloud top height and the occurrence of flashes and. The emissions are tuned to a low value of 1 Tg/yr (with an average NO_x production per cloud-to-ground flash) to achieve a realistic O_3 burden in the troposphere. The plant emissions of isoprene are modelled with the MEGAN algorithm. Different from other studies with EMAC, here the model includes the CO_2 inhibition (using the online calculated CO_2 concentration within the plants [56]. The unstressed emissions first scaled to best estimates by [57]. Then, a drought stress factor based on the CO_2 assimilation rate is applied according to [58]. Final modelled isoprene emissions for the 2018-2020 period are 329 Tg/yr, consistent with [59].

Abiotic stresses

The transpiration and dry deposition process at plants is represented with a photosynthesis scheme which describes the CO_2 assimilation of plants based on physiological considerations (here only for crops) in dependence to CO_2, temperature, radiation, available and humidity as used in the IFS model [60]. Additionally, two abiotic stressors were implemented for the purpose of this study. First, the plant response to water stress depends here on leaf water potential which have been shown to succeed over the common used soil-moisture stress factor [26, 61, 62]. The O_3-induced damage, based on [63], assesses the O_3 flux derived from the multiple resistance scheme [64, 65] against the phytotoxic threshold. Different from other studies, we implemented a dynamical measure for this based on the gross assimilation of plants and a proportionality constant of 0.20 $\mu g(O_3)/mg(CO_2)$ [66]. To consider the limited lifetime of plants we re-set the accumulated ozone damage when the vegetation density decreases for two month. Vegetation density is pre-scribed with a monthly averages of Leaf Area Index (LAI $[m^2/m^2]$) obtained by a Moderate Resolution Imaging Spectroradiometer.

Storyline approach

To distinguish the dynamic and thermodynamic aspects of climate change and reproduce the large-scale dynamics, the horizontal winds (divergence, vorticity) are nudged in spectral space up to a level of 12 hPa at all wave numbers (up to 106 at the spatial resolution used, T106L47MA corresponding to 1.1°×1.1 °) as initially proposed by [67] towards reanalysis data of ERA5 by Newtonian relaxation. The relaxation times are between 6 and 48 h. These are numbers higher than the ones used by other studies [68, 69] and were chosen to minimise model deviation from observation data. Two specific model-set ups are needed to create the storylines: (1) The ocean is pre-scribed by synthetic sea surface temperature (SST) forcing data which represents a 2K and 2.75K higher global average temperature. To this end, we used sea and land surface temperature data simulated by the first ten members of the MPI-ESM ensemble (1850-2100). Following the approach by [70], we calculated the (SST and land) temperature anomaly of the targeted future period (2064-2073, 2090-2100) relative to a historic period (1850-1920) to yield the so called warming pattern. To eliminate the historical temperature trend from the warming pattern a weighting factor was applied yielding one global 'future' SST field per month. The 2m temperature anomaly relative to the pre-industrial period 1850-1920 and the SST warming signal can be found in the supplement (Fig. S10). (2) The long-lived climate gases (LLCG) CO_2, CH_4, N_2O, CFC11, CFC12 are nudged with data branched off from the CCMI2-RD2 simulation performed with EMAC. The RD2 CCMI2 simulations (several members) reach a global average temperature anomaly of 2.75 K at the end of this century, following the SSP2-4.5 CMIP6 scenario, https://www.sparc-climate.org/wp-content/uploads/sites/5/2021/07/SPARCnewsletter_Jul2021_web.pdf and are the only climate simulations available from EMAC. Global average timeseries of this are shown in Figure S11. The O_3 chemistry is influenced by this. The anthropogenic emissions of short-lived gases are fixed to the emissions of 2018. Also, the future land cover is described by the LAI data for 2018 (and following years).

Ozone biases in the *factual* scenario

The comparison of tropospheric ozone with the chemical reanalysis TES [71] in Figure S9 (mean of data in 700-800 hPa) shows a mean bias of 10-20 ppb, exemplary for 2018, which is in agreement with the literature. The overestimation over the Indian ocean is due to complex cloud chemistry neglected here [72]. Additionally, high biases occur over mountain ranges (Andes, California, Mongolia) which can be linked to the limited model resolution of topography. [73] found a bias of 14 ppb on average in tropical regions and 11 ppb over the ocean. A comparison of 6 CMIP6 models with surface O_3 observations (TOAR) show a consistent overestimation of 16 ppb in most regions (NH) during the years 2005-2014 [74] similar to [75]. The global burden of 370 Tg estimated by EMAC for the factual (+1.1K vs. pre-industrial) climate

is within the multi-model estimates (330-380 Tg) from the literature [22, 75]. In comparison, EMAC yields about slightly larger chemical production and loss of ozone (see Tab. S1). Furthermore, EMAC estimates a lower dry deposition term of 780 Tg/yr (compared to 800-1000 Tg/yr, [22, 75]) due to the additional environmental stressors (see Sec. A.1).

A.2 Assessment of Premature Morality

We determined the premature mortality number associated with ground-level ozone by applying health impact functions that link variations in air pollution levels to shifts in mortality. The global ground-level ozone concentrations we used is simulated by the global atmospheric chemistry model ECHAM/MESSy. Health impact functions for ozone are constructed based on a logarithmic-linear relationship between relative risk and concentrations, which is defined and widely used in epidemiological research [76, 77].

$$RR = exp[\beta(C - C_0)] \; C > C_0 \tag{A1}$$

where β is the concentration-response parameter indicating the additional all non-accidental mortality attributed per unit increase of air pollutant when it is above the threshold concentration. Here, the β value for long-term ozone exposure is 1.0% per 10 $\mu g/m^3$ in the peak-season average of daily maximum 8-hour mean ozone concentration, which is recommended by Huangfu et al.[44]. C is the simulated ground-level ozone concentration and C_0 is the recommended value by the WHO [35] air quality guidelines for long-term exposure to ozone. The attributable fraction (AF), which represents the share of the mortality burden associated with the risk factor, was defined as (A2)

$$AF = (RR - 1)/RR \tag{A2}$$

$$\Delta Mort = AF \times Pop \times BMR \tag{A3}$$

AF yields an estimate for the additional deaths (ΔMort) when multiplied by the baseline mortality rate (BMR, downloaded from https://data.worldbank.org/indicator/SP.DYN.CDRT.IN) and the exposed population size (Pop)(accessed from https://hub.worldpop.org/project/categories?id=3).

References

[1] Fleming, Z.L., Doherty, R.M., Von Schneidemesser, E., Malley, C.S., Cooper, O.R., Pinto, J.P., Colette, A., Xu, X., Simpson, D., Schultz, M.G., *et al.*: Tropospheric Ozone Assessment Report: Present-day ozone distribution and trends relevant to human health. Elementa: Science of the Anthropocene (2018). https://doi.org/10.1525/elementa.273

[2] Emberson, L.D., Pleijel, H., Ainsworth, E.A., van den Berg, M., Ren, W., Osborne, S., Mills, G., Pandey, D., Dentener, F., Büker, P., Ewert, F.,

Koeble, R., Van Dingenen, R.: Ozone effects on crops and consideration in crop models. European Journal of Agronomy **100**, 19–34 (2018). https://doi.org/10.1016/j.eja.2018.06.002. Accessed 2022-07-28

[3] Monks, P.S., Archibald, A.T., Colette, A., Cooper, O., Coyle, M., Derwent, R., Fowler, D., Granier, C., Law, K.S., Mills, G.E., Stevenson, D.S., Tarasova, O., Thouret, V., von Schneidemesser, E., Sommariva, R., Wild, O., Williams, M.L.: Tropospheric ozone and its precursors from the urban to the global scale from air quality to short-lived climate forcer. Atmospheric Chemistry and Physics **15**(15), 8889–8973 (2015). https://doi.org/10.5194/acp-15-8889-2015

[4] Pope, R.J., Kerridge, B.J., Chipperfield, M.P., Siddans, R., Latter, B.G., Ventress, L.J., Pimlott, M.A., Feng, W., Comyn-Platt, E., Hayman, G.D., Arnold, S.R., Graham, A.M.: Investigation of the summer 2018 European ozone air pollution episodes using novel satellite data and modelling. Atmospheric Chemistry and Physics **23**(20), 13235–13253 (2023). https://doi.org/10.5194/acp-23-13235-2023. Publisher: Copernicus GmbH. Accessed 2023-10-23

[5] Otero, N., Sillmann, J., Schnell, J.L., Rust, H.W., Butler, T.: Synoptic and meteorological drivers of extreme ozone concentrations over Europe. Environmental Research Letters **11**(2), 024005 (2016). https://doi.org/10.1088/1748-9326/11/2/024005. Publisher: IOP Publishing. Accessed 2024-01-22

[6] Pusede, S.E., Steiner, A.L., Cohen, R.C.: Temperature and Recent Trends in the Chemistry of Continental Surface Ozone. Chemical Reviews **115**(10), 3898–3918 (2015). https://doi.org/10.1021/cr5006815. Publisher: American Chemical Society. Accessed 2023-06-28

[7] Tawfik, A.B., Steiner, A.L.: A proposed physical mechanism for ozone-meteorology correlations using land–atmosphere coupling regimes. Atmospheric Environment **72**, 50–59 (2013). https://doi.org/10.1016/j.atmosenv.2013.03.002. Accessed 2022-05-24

[8] Clifton, O.E., Fiore, A.M., Massman, W.J., Baublitz, C.B., Coyle, M., Emberson, L., Fares, S., Farmer, D.K., Gentine, P., Gerosa, G., Guenther, A.B., Helmig, D., Lombardozzi, D.L., Munger, J.W., Patton, E.G., Pusede, S.E., Schwede, D.B., Silva, S.J., Sörgel, M., Steiner, A.L., Tai, A.P.K.: Dry Deposition of Ozone Over Land: Processes, Measurement, and Modeling. Reviews of Geophysics **58**(1), 2019–000670 (2020). https://doi.org/10.1029/2019RG000670

[9] Grote, R., Lavoir, A.-V., Rambal, S., Staudt, M., Zimmer, I., Schnitzler, J.-P.: Modelling the drought impact on monoterpene fluxes from an evergreen Mediterranean forest canopy. Oecologia **160**(2), 213–223 (2009).

https://doi.org/10.1007/s00442-009-1298-9. Publisher: Springer

[10] Zanis, P., Akritidis, D., Turnock, S., Naik, V., Szopa, S., Georgoulias, A.K., Bauer, S.E., Deushi, M., Horowitz, L.W., Keeble, J., Le Sager, P., O'Connor, F.M., Oshima, N., Tsigaridis, K., Van Noije, T.: Climate change penalty and benefit on surface ozone: a global perspective based on CMIP6 earth system models. Environmental Research Letters **17**(2), 024014 (2022). https://doi.org/10.1088/1748-9326/ac4a34. Accessed 2023-09-20

[11] Griffiths, P.T., Keeble, J., Shin, Y.M., Abraham, N.L., Archibald, A.T., Pyle, J.A.: On the Changing Role of the Stratosphere on the Tropospheric Ozone Budget: 1979–2010. Geophysical Research Letters **47**(10), 2019–086901 (2020). https://doi.org/10.1029/2019GL086901

[12] Shepherd, T.G.: Atmospheric circulation as a source of uncertainty in climate change projections. Nature Geoscience **7**(10), 703–708 (2014). https://doi.org/10.1038/ngeo2253. Number: 10 Publisher: Nature Publishing Group. Accessed 2024-02-05

[13] Shepherd, T.G., Boyd, E., Calel, R.A., Chapman, S.C., Dessai, S., Dima-West, I.M., Fowler, H.J., James, R., Maraun, D., Martius, O., *et al.*: Storylines: an alternative approach to representing uncertainty in physical aspects of climate change. Climatic change **151**(3), 555–571 (2018). https://doi.org/10.1007/s10584-018-2317-9. Publisher: Springer

[14] Rousi, E., Fink, A.H., Andersen, L.S., Becker, F.N., Beobide-Arsuaga, G., Breil, M., Cozzi, G., Heinke, J., Jach, L., Niermann, D., Petrovic, D., Richling, A., Riebold, J., Steidl, S., Suarez-Gutierrez, L., Tradowsky, J.S., Coumou, D., Düsterhus, A., Ellsäßer, F., Fragkoulidis, G., Gliksman, D., Handorf, D., Haustein, K., Kornhuber, K., Kunstmann, H., Pinto, J.G., Warrach-Sagi, K., Xoplaki, E.: The extremely hot and dry 2018 summer in central and northern Europe from a multi-faceted weather and climate perspective. Natural Hazards and Earth System Sciences **23**(5), 1699–1718 (2023). https://doi.org/10.5194/nhess-23-1699-2023. Accessed 2023-05-14

[15] Vautard, R., Aalst, M.v., Boucher, O., Drouin, A., Haustein, K., Kreienkamp, F., Oldenborgh, G.J.v., Otto, F.E.L., Ribes, A., Robin, Y., Schneider, M., Soubeyroux, J.-M., Stott, P., Seneviratne, S.I., Vogel, M.M., Wehner, M.: Human contribution to the record-breaking June and July 2019 heatwaves in Western Europe. Environmental Research Letters **15**(9), 094077 (2020). https://doi.org/10.1088/1748-9326/aba3d4. Publisher: IOP Publishing. Accessed 2024-02-14

[16] Blunden, J., Boyer, T.: State of the Climate in 2020. Bulletin of the American Meteorological Society **102**(8), 1–475 (2021). https://doi.org/

10.1175/2021BAMSStateoftheClimate.1. Publisher: American Meteorological Society Section: Bulletin of the American Meteorological Society. Accessed 2024-02-14

[17] Seneviratne, S.I., Corti, T., Davin, E.L., Hirschi, M., Jaeger, E.B., Lehner, I., Orlowsky, B., Teuling, A.J.: Investigating soil moisture–climate interactions in a changing climate: A review. Earth-Science Reviews **99**(3), 125–161 (2010). https://doi.org/10.1016/j.earscirev.2010.02.004. Accessed 2023-06-18

[18] Dirmeyer, P.A., Balsamo, G., Blyth, E.M., Morrison, R., Cooper, H.M.: Land-Atmosphere Interactions Exacerbated the Drought and Heatwave Over Northern Europe During Summer 2018. AGU Advances **2**(2), 2020–000283 (2021). https://doi.org/10.1029/2020AV000283. _eprint: https://onlinelibrary.wiley.com/doi/pdf/10.1029/2020AV000283. Accessed 2023-05-14

[19] Lin, M., Horowitz, L.W., Xie, Y., Paulot, F., Malyshev, S., Shevliakova, E., Finco, A., Gerosa, G., Kubistin, D., Pilegaard, K.: Vegetation feedbacks during drought exacerbate ozone air pollution extremes in Europe. Nature Climate Change **10**(5), 444–451 (2020). https://doi.org/10.1038/s41558-020-0743-y. Number: 5 Publisher: Nature Publishing Group. Accessed 2022-05-17

[20] Jöckel, P., Kerkweg, A., Pozzer, A., Sander, R., Tost, H., Riede, H., Baumgaertner, A., Gromov, S., Kern, B.: Development cycle 2 of the Modular Earth Submodel System (MESSy2). Geoscientific Model Development **3**(2), 717–752 (2010). https://doi.org/10.5194/gmd-3-717-2010. Publisher: Copernicus GmbH. Accessed 2022-12-09

[21] Piotrowicz, S.R., Bezdek, H.F., Harvey, G.R., Springer-young, M., Hanson, K.J.: On the ozone minimum over the equatorial Pacific Ocean. Journal of Geophysical Research: Atmospheres **96**(D10), 18679–18687 (1991). https://doi.org/10.1029/91JD01809. _eprint: https://onlinelibrary.wiley.com/doi/pdf/10.1029/91JD01809. Accessed 2024-03-08

[22] Griffiths, P.T., Murray, L.T., Zeng, G., Shin, Y.M., Abraham, N.L., Archibald, A.T., Deushi, M., Emmons, L.K., Galbally, I.E., Hassler, B., Horowitz, L.W., Keeble, J., Liu, J., Moeini, O., Naik, V., O'Connor, F.M., Oshima, N., Tarasick, D., Tilmes, S., Turnock, S.T., Wild, O., Young, P.J., Zanis, P.: Tropospheric ozone in CMIP6 simulations. Atmospheric Chemistry and Physics **21**(5), 4187–4218 (2021). https://doi.org/10.5194/acp-21-4187-2021. Publisher: Copernicus GmbH. Accessed 2022-07-06

[23] Heald, C.L., Wilkinson, M.J., Monson, R.K., Alo, C.A., Wang, G., Guenther, A.: Response of isoprene emission to ambient CO2

changes and implications for global budgets. Global Change Biology **15**(5), 1127–1140 (2009). https://doi.org/10.1111/j.1365-2486.2008.01802.x. _eprint: https://onlinelibrary.wiley.com/doi/pdf/10.1111/j.1365-2486.2008.01802.x. Accessed 2023-02-28

[24] Tai, A.P.K., Mickley, L.J., Heald, C.L., Wu, S.: Effect of CO2 inhibition on biogenic isoprene emission: Implications for air quality under 2000 to 2050 changes in climate, vegetation, and land use. Geophysical Research Letters **40**(13), 3479–3483 (2013). https://doi.org/10.1002/grl.50650. _eprint: https://onlinelibrary.wiley.com/doi/pdf/10.1002/grl.50650. Accessed 2024-03-08

[25] Vicente-Serrano, S.M., Miralles, D.G., McDowell, N., Brodribb, T., Domínguez-Castro, F., Leung, R., Koppa, A.: The uncertain role of rising atmospheric CO2 on global plant transpiration. Earth-Science Reviews **230**, 104055 (2022). https://doi.org/10.1016/j.earscirev.2022.104055. Accessed 2023-01-09

[26] Emmerichs, T., Lu, Y.-S., Taraborrelli, D.: The importance of plant-water stress for predictions of ground-level ozone in a warm world. https://www.semanticscholar.org/paper/The-importance-of-plant-water-stress-for-of-ozone-a-Emmerichs-Lu/3e3cd9a076611be8606bd9198f182491057d6aa4 Accessed 2024-01-22

[27] Auvray, M., Bey, I.: Long-range transport to Europe: Seasonal variations and implications for the European ozone budget. Journal of Geophysical Research: Atmospheres **110**(D11) (2005). https://doi.org/10.1029/2004JD005503. _eprint: https://onlinelibrary.wiley.com/doi/pdf/10.1029/2004JD005503. Accessed 2024-03-06

[28] Monks, P.S.: Gas-phase radical chemistry in the troposphere. Chemical Society Reviews **34**(5), 376 (2005). https://doi.org/10.1039/b307982c. Accessed 2022-07-05

[29] Rasmussen, D.J., Hu, J., Mahmud, A., Kleeman, M.J.: The Ozone–Climate Penalty: Past, Present, and Future. Environmental Science & Technology **47**(24), 14258–14266 (2013). https://doi.org/10.1021/es403446m. Publisher: American Chemical Society. Accessed 2023-12-15

[30] Mo, Z., Shao, M., Wang, W., Liu, Y., Wang, M., Lu, S.: Evaluation of biogenic isoprene emissions and their contribution to ozone formation by ground-based measurements in Beijing, China. Science of the Total Environment **627**, 1485–1494 (2018). https://doi.org/10.1016/j.scitotenv.2018.01.336

[31] Kavassalis, S.C., Murphy, J.G.: Understanding ozone-meteorology correlations: A role for dry deposition. Geophysical Research Letters **44**(6), 2922–2931 (2017). https://doi.org/10.1002/2016GL071791. Publisher: Wiley Online Library

[32] Hyo-Jung, L., Lim-Seok, C., Jaffe, D.A., Bak, J., Liu, X., Abad, G.G., Hyun-Young, J., Yu-Jin, J., Lee, J.-B., Cheol-Hee, K.: Ozone Continues to Increase in East Asia Despite Decreasing NO2: Causes and Abatements. Remote Sensing **13**(11) (2021). https://doi.org/10.3390/rs13112177. Place: Basel, Switzerland Publisher: MDPI AG. Accessed 2024-03-27

[33] Hu, X.-M., Sigler, J., Fuentes, J.: Variability of ozone in the marine boundary layer of the equatorial Pacific Ocean. Journal of Atmospheric Chemistry **66**, 117–136 (2010). https://doi.org/10.1007/s10874-011-9196-z

[34] Porter, W.C., Heald, C.L.: The mechanisms and meteorological drivers of the summertime ozone–temperature relationship. Atmospheric Chemistry and Physics **19**(21), 13367–13381 (2019). https://doi.org/10.5194/acp-19-13367-2019

[35] (WHO), W.H.O.: WHO air quality guidelines. Particulate matter (PM 2.5 and PM 10), ozone, nitrogen dioxide, sulfur dioxide and carbon monoxide. https://iris.who.int/bitstream/handle/10665/345329/9789240034228-eng.pdf?sequence=1&isAllowed=y Accessed 2024-03-11

[36] Gao, M., Gao, J., Zhu, B., Kumar, R., Lu, X., Song, S., Zhang, Y., Jia, B., Wang, P., Beig, G., Hu, J., Ying, Q., Zhang, H., Sherman, P., McElroy, M.B.: Ozone pollution over China and India: seasonality and sources. Atmospheric Chemistry and Physics **20**(7), 4399–4414 (2020). https://doi.org/10.5194/acp-20-4399-2020. Publisher: Copernicus GmbH. Accessed 2024-03-06

[37] Iturbide, M., Gutiérrez, J.M., Alves, L.M., Bedia, J., Cerezo-Mota, R., Cimadevilla, E., Cofiño, A.S., Di Luca, A., Faria, S.H., Gorodetskaya, I.V., Hauser, M., Herrera, S., Hennessy, K., Hewitt, H.T., Jones, R.G., Krakovska, S., Manzanas, R., Martínez-Castro, D., Narisma, G.T., Nurhati, I.S., Pinto, I., Seneviratne, S.I., van den Hurk, B., Vera, C.S.: An update of IPCC climate reference regions for subcontinental analysis of climate model data: definition and aggregated datasets. Earth System Science Data **12**(4), 2959–2970 (2020). https://doi.org/10.5194/essd-12-2959-2020. Accessed 2023-03-21

[38] Sadiq, M., Tai, A.P.K., Lombardozzi, D., Val Martin, M.: Effects of ozone–vegetation coupling on surface ozone air quality via biogeochemical and meteorological feedbacks. Atmospheric Chemistry and Physics **17**(4), 3055–3066 (2017). https://doi.org/10.5194/acp-17-3055-2017. Accessed

2022-03-14

[39] Lombardozzi, D., Levis, S., Bonan, G., Hess, P.G., Sparks, J.P.: The Influence of Chronic Ozone Exposure on Global Carbon and Water Cycles. Journal of Climate **28**(1), 292–305 (2015). https://doi.org/10.1175/JCLI-D-14-00223.1. Publisher: American Meteorological Society Section: Journal of Climate. Accessed 2022-07-28

[40] Tai, A.P.K., Sadiq, M., Pang, J.Y.S., Yung, D.H.Y., Feng, Z.: Impacts of Surface Ozone Pollution on Global Crop Yields: Comparing Different Ozone Exposure Metrics and Incorporating Co-effects of CO2. Frontiers in Sustainable Food Systems **5** (2021). Accessed 2022-07-13

[41] Ceppi, P., Gregory, J.M.: Relationship of tropospheric stability to climate sensitivity and Earth's observed radiation budget. Proceedings of the National Academy of Sciences **114**(50), 13126–13131 (2017). https://doi.org/10.1073/pnas.1714308114. Publisher: Proceedings of the National Academy of Sciences. Accessed 2024-02-20

[42] Malashock, D.A., DeLang, M.N., Becker, J.S., Serre, M.L., West, J.J., Chang, K.-L., Cooper, O.R., Anenberg, S.C.: Estimates of ozone concentrations and attributable mortality in urban, peri-urban and rural areas worldwide in 2019. Environmental Research Letters **17**(5), 054023 (2022). https://doi.org/10.1088/1748-9326/ac66f3. Publisher: IOP Publishing. Accessed 2024-03-19

[43] GBD 2019 Risk Factors Collaborators: Global burden of 87 risk factors in 204 countries and territories, 1990-2019: a systematic analysis for the Global Burden of Disease Study 2019. Lancet (London, England) **396**(10258), 1223–1249 (2020). https://doi.org/10.1016/S0140-6736(20)30752-2

[44] Huangfu, P., Atkinson, R.: Long-term exposure to NO2 and O3 and all-cause and respiratory mortality: A systematic review and meta-analysis. Environment International **144**, 105998 (2020). https://doi.org/10.1016/j.envint.2020.105998. Accessed 2024-03-19

[45] Turner, M.C., Jerrett, M., Pope, C.A., Krewski, D., Gapstur, S.M., Diver, W.R., Beckerman, B.S., Marshall, J.D., Su, J., Crouse, D.L., Burnett, R.T.: Long-Term Ozone Exposure and Mortality in a Large Prospective Study. American Journal of Respiratory and Critical Care Medicine **193**(10), 1134–1142 (2016). https://doi.org/10.1164/rccm.201508-1633OC

[46] Akritidis, D., Bacer, S., Zanis, P., Georgoulias, A., Chowdhury, S., Horowitz, L., Naik, V., O'Connor, F., Keeble, J., Sager, P., Noije, T., Zhou, P., Turnock, S., West, J., Lelieveld, J., Pozzer, A.: Strong increase

in mortality attributable to ozone pollution under a climate change and demographic scenario. Environmental Research Letters **19** (2024). https://doi.org/10.1088/1748-9326/ad2162

[47] Silva, R.A., West, J.J., Lamarque, J.-F., Shindell, D.T., Collins, W.J., Dalsoren, S., Faluvegi, G., Folberth, G., Horowitz, L.W., Nagashima, T., Naik, V., Rumbold, S.T., Sudo, K., Takemura, T., Bergmann, D., Cameron-Smith, P., Cionni, I., Doherty, R.M., Eyring, V., Josse, B., MacKenzie, I.A., Plummer, D., Righi, M., Stevenson, D.S., Strode, S., Szopa, S., Zeng, G.: The effect of future ambient air pollution on human premature mortality to 2100 using output from the ACCMIP model ensemble. Atmospheric Chemistry and Physics **16**(15), 9847–9862 (2016). https://doi.org/10.5194/acp-16-9847-2016

[48] Krause, D.: JUWELS: Modular Tier-0/1 Supercomputer at the Jülich Supercomputing Centre. Journal of large-scale research facilities JLSRF **5**, 135–135 (2019). https://doi.org/10.17815/jlsrf-5-171. Accessed 2024-03-15

[49] Jülich Supercomputing Centre: JURECA: Modular supercomputer at Jülich Supercomputing Centre. Journal of large-scale research facilities **4**(A132) (2018). https://doi.org/10.17815/jlsrf-4-121-1

[50] Roeckner, E., Bäuml, G., Bonaventura, L., Brokopf, R., Esch, M., Giorgetta, M., Hagemann, S., Kirchner, I., Kornblueh, L., Manzini, E., et al.: The atmospheric general circulation model ECHAM 5. PART I: Model description. MPI report (2003). Publisher: Max-Planck-Institut für Meteorologie

[51] Sander, R., Baumgaertner, A., Cabrera-Perez, D., Frank, F., Gromov, S., Grooß, J.-U., Harder, H., Huijnen, V., Jöckel, P., Karydis, V.A., *et al.*: The community atmospheric chemistry box model CAABA/MECCA-4.0. Geoscientific model development **12**(4), 1365–1385 (2019). https://doi.org/10.5194/gmd-12-1365-2019. Publisher: Copernicus Publications

[52] Jöckel, P., Tost, H., Pozzer, A., Kunze, M., Kirner, O., Brenninkmeijer, C.A.M., Brinkop, S., Cai, D.S., Dyroff, C., Eckstein, J., Frank, F., Garny, H., Gottschaldt, K.-D., Graf, P., Grewe, V., Kerkweg, A., Kern, B., Matthes, S., Mertens, M., Meul, S., Neumaier, M., Nützel, M., Oberländer-Hayn, S., Ruhnke, R., Runde, T., Sander, R., Scharffe, D., Zahn, A.: Earth System Chemistry integrated Modelling (ESCiMo) with the Modular Earth Submodel System (MESSy) version 2.51. Geoscientific Model Development **9**(3), 1153–1200 (2016). https://doi.org/10.5194/gmd-9-1153-2016

[53] Gromov, S., Jöckel, P., Sander, R., Brenninkmeijer, C.A.M.: A kinetic chemistry tagging technique and its application to modelling the

stable isotopic composition of atmospheric trace gases. Geoscientific Model Development **3**(2), 337–364 (2010). https://doi.org/10.5194/gmd-3-337-2010

[54] Pringle, K.J., Tost, H., Message, S., Steil, B., Giannadaki, D., Nenes, A., Fountoukis, C., Stier, P., Vignati, E., Lelieveld, J.: Description and evaluation of GMXe: a new aerosol submodel for global simulations (v1). Geoscientific Model Development **3**(2), 391–412 (2010). https://doi.org/10.5194/gmd-3-391-2010. Publisher: Copernicus GmbH. Accessed 2024-01-22

[55] Rosanka, S., Tost, H., Sander, R., Jöckel, P., Kerkweg, A., Taraborrelli, D.: How Non-equilibrium Aerosol Chemistry Impacts Particle Acidity: the GMXe AERosol CHEMistry (GMXe–AERCHEM, V1.0) Sub-submodel of MESSy, (2023). https://doi.org/10.5194/egusphere-2023-2587

[56] Guenther, A.B., Jiang, X., Heald, C.L., Sakulyanontvittaya, T., Duhl, T., Emmons, L.K., Wang, X.: The Model of Emissions of Gases and Aerosols from Nature version 2.1 (MEGAN2.1): an extended and updated framework for modeling biogenic emissions. Geoscientific Model Development **5**(6), 1471–1492 (2012). https://doi.org/10.5194/gmd-5-1471-2012

[57] Sindelarova, K., Markova, J., Simpson, D., Huszar, P., Karlicky, J., Darras, S., Granier, C.: High-resolution biogenic global emission inventory for the time period 2000–2019 for air quality modelling. Earth System Science Data **14**(1), 251–270 (2022). https://doi.org/10.5194/essd-14-251-2022. Publisher: Copernicus GmbH. Accessed 2022-07-15

[58] Jiang, X., Guenther, A., Potosnak, M., Geron, C., Seco, R., Karl, T., Kim, S., Gu, L., Pallardy, S.: Isoprene emission response to drought and the impact on global atmospheric chemistry. Atmospheric Environment **183**, 69–83 (2018). https://doi.org/10.1016/j.atmosenv.2018.01.026. Publisher: Elsevier

[59] Müller, J.-F., Stavrakou, T., Wallens, S., De Smedt, I., Van Roozendael, M., Potosnak, M.J., Rinne, J., Munger, B., Goldstein, A., Guenther, A.B.: Global isoprene emissions estimated using MEGAN, ECMWF analyses and a detailed canopy environment model. Atmospheric Chemistry and Physics **8**(5), 1329–1341 (2008). https://doi.org/10.5194/acp-8-1329-2008

[60] ECMWF: IFS Documentation CY47R3. IFS Documentation. ECMWF, ??? (2021)

[61] Verhoef, A., Egea, G.: Modeling plant transpiration under limited soil water: Comparison of different plant and soil hydraulic parameterizations

and preliminary implications for their use in land surface models. Agricultural and Forest Meteorology **191**, 22–32 (2014). https://doi.org/10.1016/j.agrformet.2014.02.009. Accessed 2022-04-26

[62] Kennedy, D., Swenson, S., Oleson, K.W., Lawrence, D.M., Fisher, R., Lola da Costa, A.C., Gentine, P.: Implementing Plant Hydraulics in the Community Land Model, Version 5. Journal of Advances in Modeling Earth Systems **11**(2), 485–513 (2019). https://doi.org/10.1029/2018MS001500. _eprint: https://onlinelibrary.wiley.com/doi/pdf/10.1029/2018MS001500. Accessed 2022-08-03

[63] Lombardozzi, D., Sparks, J.P., Bonan, G., Levis, S.: Ozone exposure causes a decoupling of conductance and photosynthesis: implications for the Ball-Berry stomatal conductance model. Oecologia **169**(3), 651–659 (2012). https://doi.org/10.1007/s00442-011-2242-3. Accessed 2022-08-18

[64] Wesely, M.: Parameterization of surface resistances to gaseous dry deposition in regional-scale numerical models. Atmospheric Environment (1967) **23**(6), 1293–1304 (1989). https://doi.org/10.1016/0004-6981(89)90153-4. Publisher: Elsevier

[65] Emmerichs, T., Kerkweg, A., Ouwersloot, H., Fares, S., Mammarella, I., Taraborrelli, D.: A revised dry deposition scheme for land–atmosphere exchange of trace gases in ECHAM/MESSy v2.54. Geoscientific Model Development **14**(1), 495–519 (2021). https://doi.org/10.5194/gmd-14-495-2021. Publisher: Copernicus GmbH. Accessed 2021-06-16

[66] Massman, W.J.: Toward an ozone standard to protect vegetation based on effective dose: a review of deposition resistances and a possible metric. Atmospheric Environment **38**(15), 2323–2337 (2004). https://doi.org/10.1016/j.atmosenv.2003.09.079. Accessed 2022-12-13

[67] Jeuken, A.B.M., Siegmund, P.C., Heijboer, L.C., Feichter, J., Bengtsson, L.: On the potential of assimilating meteorological analyses in a global climate model for the purpose of model validation. Journal of Geophysical Research: Atmospheres **101**(D12), 16939–16950 (1996). https://doi.org/10.1029/96JD01218

[68] Sánchez-Benítez, A., Goessling, H., Pithan, F., Semmler, T., Jung, T.: The July 2019 European Heat Wave in a Warmer Climate: Storyline Scenarios with a Coupled Model Using Spectral Nudging. Journal of Climate **35**(8), 2373–2390 (2022). https://doi.org/10.1175/JCLI-D-21-0573.1. Publisher: American Meteorological Society Section: Journal of Climate. Accessed 2022-04-06

[69] van Garderen, L., Feser, F., Shepherd, T.G.: A methodology for attributing the role of climate change in extreme events: a global spectrally nudged storyline. Natural Hazards and Earth System Sciences **21**(1), 171–186 (2021). https://doi.org/10.5194/nhess-21-171-2021. Publisher: Copernicus GmbH. Accessed 2022-08-18

[70] van Garderen, L.: Climate change attribution of extreme weather events using spectrally nudged event storylines. doctoralThesis, Staats- und Universitätsbibliothek Hamburg Carl von Ossietzky (2022). Accepted: 2022-12-15T11:06:27Z. https://ediss.sub.uni-hamburg.de/handle/ediss/9978 Accessed 2024-02-07

[71] Miyazaki, K., Bowman, K., Sekiya, T., Eskes, H., Boersma, F., Worden, H., Livesey, N., Payne, V.H. V. H., Sudo, K., Kanaya, Y., Takigawa, M., Ogochi, K.: Chemical Reanalysis Products. Jet Propulsion Laboratory (2019). https://doi.org/10.25966/9qgv-fe81. https://tes.jpl.nasa.gov/tes/chemical-reanalysis/ Accessed 2024-03-11

[72] Rosanka, S., Sander, R., Franco, B., Wespes, C., Wahner, A., Taraborrelli, D.: Oxidation of low-molecular-weight organic compounds in cloud droplets: global impact on tropospheric oxidants. Atmospheric Chemistry and Physics **21**(12), 9909–9930 (2021). https://doi.org/10.5194/acp-21-9909-2021. Accessed 2024-03-08

[73] Brown, F., Folberth, G.A., Sitch, S., Bauer, S., Bauters, M., Boeckx, P., Cheesman, A.W., Deushi, M., Dos Santos Vieira, I., Galy-Lacaux, C., Haywood, J., Keeble, J., Mercado, L.M., O'Connor, F.M., Oshima, N., Tsigaridis, K., Verbeeck, H.: The ozone–climate penalty over South America and Africa by 2100. Atmospheric Chemistry and Physics **22**(18), 12331–12352 (2022). https://doi.org/10.5194/acp-22-12331-2022. Publisher: Copernicus GmbH. Accessed 2023-12-19

[74] Turnock, S.T., Allen, R.J., Andrews, M., Bauer, S.E., Deushi, M., Emmons, L., Good, P., Horowitz, L., John, J.G., Michou, M., Nabat, P., Naik, V., Neubauer, D., O'Connor, F.M., Olivié, D., Oshima, N., Schulz, M., Sellar, A., Shim, S., Takemura, T., Tilmes, S., Tsigaridis, K., Wu, T., Zhang, J.: Historical and future changes in air pollutants from CMIP6 models. Atmospheric Chemistry and Physics **20**(23), 14547–14579 (2020). https://doi.org/10.5194/acp-20-14547-2020. Publisher: Copernicus GmbH. Accessed 2023-12-19

[75] Young, P.J., Naik, V., Fiore, A.M., Gaudel, A., Guo, J., Lin, M., Neu, J., Parrish, D., Rieder, H., Schnell, J., et al.: Tropospheric Ozone Assessment Report: Assessment of global-scale model performance for global and regional ozone distributions, variability, and trends. Elem Sci Anth **6**(1) (2018). https://doi.org/10.1525/elementa.265. Publisher: University of California Press

[76] Jerrett, M., Burnett, R.T., Pope, C.A., Ito, K., Thurston, G., Krewski, D., Shi, Y., Calle, E., Thun, M.: Long-term ozone exposure and mortality. The New England Journal of Medicine **360**(11), 1085–1095 (2009). https://doi.org/10.1056/NEJMoa0803894

[77] Anenberg, S.C., Horowitz, L.W., Tong, D.Q., West, J.J.: An estimate of the global burden of anthropogenic ozone and fine particulate matter on premature human mortality using atmospheric modeling. Environmental Health Perspectives **118**(9), 1189–1195 (2010). https://doi.org/10.1289/ehp.0901220

Supplementary Files

This is a list of supplementary files associated with this preprint. Click to download.

- FigS1.jpg
- FigS2.jpg
- FigS3.jpg
- FigS4.jpg
- FigS5.jpg
- FigS6.jpg
- FigS7.jpg
- FigS8.jpg
- FigS9.jpg